## **Turkish Computational and Theoretical Chemistry**

Turkish Comp Theo Chem (TC&TC)



e-ISSN: 2602-3237

https://doi.org/10.33435/tcandtc.1628962

Received: 29.01.2025 Accepted: 04.05.2025 Research Article

Molecular Docking and Molecular Dynamic Simulation of New Single Guide RNA From Tail

Fiber Gene (Gp019) Bacteriophage Salmonella

Erlia Narulita<sup>a,b,c,l</sup>, Aisa Aulia Nur Aini<sup>a,d</sup>, Hardian Susilo Addy<sup>a,c,d</sup>, Riska Ayu Febrianti<sup>d</sup>

<sup>a</sup>Postgraduate of Biotechnology, Graduate School, University of Jember, Jember, Indonesia <sup>b</sup>Department of Biology Education, Faculty of Teacher Training and Education, University of Jember, Jember, Indonesia

<sup>c</sup>Department of Agrotechnology, Faculty of Agriculture, University of Jember, Jember, Indonesia <sup>d</sup>Center for Development of Advance Science and Technology, University of Jember, Jember, Indonesia

Abstract: In this study, we designed in-silico single guide RNA (sgRNA) as the initial step of the genome editing process using the CRISPR-Cas9 system on the Salmonella SSE-121 phage. The target gene encodes a tail fiber protein, which is essential for recognizing and attaching to host bacteria. Conducting in-silico sgRNA design aims to identify optimal sgRNA candidates for the Salmonella phage while minimizing potential failures. The genome sequence of the Salmonella phage was retrieved from NCBI, and Cas9 protein data was obtained from the RCSB Protein Data Bank (PDB). Using CHOPCHOP, sgRNA predictions resulted in 439 candidates. These candidates were evaluated based on efficiency scores, GC content, and self-complementarity, leading to the selection of 58 sgRNA candidates. Further refinement of these candidates involved docking score assessments through the HNADOCK website, narrowing the selection to 33 sgRNA candidates, which were subsequently re-docked with the Cas9 protein using the HDOCK website. The five best sgRNA candidates were validated to determine the most optimal sgRNA. Plasmid construction was performed by aligning the plasmid structure with the selected sgRNA for subsequent in-vivo studies. The docking scores obtained were -553.09 for sgRNA and target DNA binding, and -399.18 for sgRNA and Cas9 binding. Molecular dynamics simulations analyzing sgRNA and Cas9 protein interactions—including hydrogen bonding, RMSD, RMSF, and RG—demonstrated structural stability throughout the simulation. The plasmid construct pCMV-T7-ABE8 exhibited effective binding with sgRNA candidate 15 when using the SnaBI restriction enzyme. In conclusion, sgRNA candidate 15 emerged as the most optimal choice for the CRISPR-Cas9 system, enabling precise modifications of the Salmonella phage genome.

Keywords: CRISPR, genome editing, sgRNA, bacteriophage, Salmonella

## 1. Introduction

Foodborne diseases, caused by microbial contamination of food, are a major health issue globally. According to data from the World Health Organization (WHO), contaminated food is responsible for more than 600 million cases annually (nearly 1 in 10 people worldwide). The most common causes of foodborne diseases are pathogenic bacteria such as Salmonella, Vibrio parahaemolyticus, Listeria monocytogenes, Staphylococcus aureus, and several other pathogens

[1]. Salmonella, particularly S. enterica, is a pathogenic bacteria that plays a significant role in infecting humans and causing diseases linked to contamination from poultry products, dairy, seafood, and vegetables [2], [3]. This bacteria is responsible for approximately 94 million cases of Salmonellosis annually and has caused around 155,000 deaths worldwide [4].

Efforts to reduce food poisoning caused by pathogenic bacteria such as Salmonella typically involve therapy and treatment with antibiotics.

e-mail: erlia.fkip@unej.ac.id

<sup>&</sup>lt;sup>1</sup> Corresponding Authors

However, this approach has the drawback of fostering bacterial resistance to antibiotics. In Salmonella, antibiotic resistance is mediated through various mechanisms, with inactivation being the most common. In this process, the antibiotic agent is destroyed or inactivated through chemical modifications catalyzed by enzymes, including reactions such as acetylation, phosphorylation, and adenylation [5]. Antibiotic resistance in Salmonella is a serious health concern, responsible for 250,000 cases in patients within the United States and posing a global threat [6].

Another approach to reducing the infection rate of Salmonella bacteria involves the use bacteriophages. These viruses have the ability to disrupt bacterial metabolism and induce cell lysis. Moreover, bacteriophages bind to specific receptors on bacterial cells, which helps minimize side effects on host cells. This specificity offers a significant advantage in the treatment of bacterial infections [7]. Salmonella phage vB\_SenM-PA13076 has been demonstrated to be both effective and safe as a bacteriophage therapy in mice [8]. In other research, bacteriophage therapy has been developed for the poultry industry to address various issues, including the prevention of Salmonella infections in eggs from different farming methods and gastrointestinal diseases caused by Salmonella spp., Campylobacter spp., and E. coli [9], [10]. This is supported by data on the application of bacteriophages in China to combat bacterial infections. Animals infected with bacteria at a minimum lethal dose were able to survive when injected with bacteriophages 15 minutes after infection [11]. However, the use of bacteriophages as a therapeutic agent has limitations due to the presence of diverse serovars in both bacteria and bacteriophages. Addressing these limitations requires the application of advanced genome editing technology to produce the desired recombinant bacteriophage.

Genome editing technology is a versatile technique used to modify the DNA sequence of a genome into a desired recombinant gene. One of the frequently used genome editing technologies is Clustered Regular Interspaced Short Palindromic Repeats-Associated Protein 9 (CRISPR-Cas9). This system has been widely applied for genome editing and gene modification in eukaryotic and prokaryotic

cells. This technology makes it possible to modify gene sequences specifically using single guide RNA (sgRNA). By using sgRNA, the CRISPR system can be utilized to identify drug target genes or disease resistance genes[12], [13]. The synthesis of sgRNA is achieved by combining crRNA and tracrRNA sequences. The resulting sgRNA plays a crucial role in recognizing specific target sequence pairs and signaling Cas9 to cleave the double-strand DNA using the double-strand break (DSB) mechanism, enabling gene editing through the CRISPR-Cas9 system [14]. This study also included an analysis of the molecular dynamics between the designed sgRNA and the Cas9 protein. Molecular dynamics is a computational method for modeling molecular systems and studying their dynamics and temporal evolution [15]. Based on this framework, this research aims to construct target sgRNA from the bacteriophage genome and examine its interaction with the Cas9 protein in the CRISPR-Cas9 system, as well as its interaction with target DNA, using various applications and supporting tools.

## 2. Computational Method

# 2.1. Whole genome sequence and target gene retrieval

Salmonella phage whole genome sequences were retrieved from the NCBI Genbank database. This study used Salmonella phage SSE-121 with accession number ID: NC\_027351. This genome sequence has a length of 144745 bp and was taken in the form of a FASTA file. The target gene used is the gene encoding the tail fiber protein of Salmonella phage SSE121 with Gene ID: 24638794. This gene is located between sequences 13752 to 16508 bp with locus tag ACQ19 gp019.

## 2.2. Cas9 protein data collection

Cas9 protein was obtained from the RSCB PDB protein bank (<a href="https://www.rcsb.org/">https://www.rcsb.org/</a>). The Cas9 protein used was isolated from *Streptococcus pyogenes* (SpyCas9) and is identified under the PDB code 4ZT0 [16].

## 2.3. Single guide RNA (sgRNA) design

The FASTA file of the Salmonella phage SSE-121 genome was uploaded to the CHOPCHOP website (<a href="https://chopchop.cbu.uib.no/">https://chopchop.cbu.uib.no/</a>), where the target gene with ID AQC19-gp019 was selected to

identify available sgRNAs for CRISPR-Cas9 genome editing. This software allows filtering of sgRNA targets based on GC content (10-90%) and self-complementarity. In this study, the mean method in Microsoft Excel was used to classify the optimal sgRNA candidates. The median efficiency value of sgRNA was first selected, followed by filtering for GC content  $\geq$ 50% and a self-complementarity score  $\leq$ 0 [17], [18]. The final selected candidates were then constructed into a 3D structure.

# 2.4. Construction of single guide RNA 3D structure

Construction of the 3D structure of single guide RNA was carried out using the RNAcomposer website (https://rnacomposer.cs.put.poznan.pl/). The 3D structure was predicted using RNA sequences along with their secondary structure in dot-bracket format. Before being input into the software, the base sequence of the sgRNA was manually converted into dot-bracket format using Excel. The resulting translation was then uploaded into the software to visualize the 3D structure. The sgRNA candidates included consist of a combination of crRNA (derived from CHOPCHOP results) and tracrRNA (originating from 20nt Cas9 4ZT0 protein)[19], [20]. The results of this stage can be downloaded in PDB file format.

# 2.5. Molecular docking of sgRNA candidates with target crRNAs

We performed molecular docking analysis using the HNADOCK software, which is accessible online (<a href="http://huanglab.phys.hust.edu.cn/hnadock/">http://huanglab.phys.hust.edu.cn/hnadock/</a>) to evaluate the binding efficiency of the sgRNA candidate (crRNA + tracrRNA) with the crRNA target AQC19\_gp019 [21]. There were two columns for nucleic acid molecules that needed to be filled. The first column was provided with sgRNA data in PDB file format, while the second column contained the crRNA target as a DNA sequence. In the modeling options, RNAfold was selected for the RNA secondary structure prediction method, 'None' was chosen for the RNA-RNA interaction prediction method, and 'No' was selected for refining the top 10 complex models. Finally, the 'Submit' button was clicked to start the molecular docking process. The results were provided as docking scores, indicating the binding

of sgRNA candidates to crRNA targets, and candidates with low docking scores were selected. The docking image is visualized using the Biovia Discovery Studio application (https://discover.3ds.com/).

# 2.6. Molecular docking of sgRNA candidate with Cas9 protein

Molecular docking between the Cas9 protein and the sgRNA candidate was conducted using the **HDOCK** webserver (http://hdock.phys.hust.edu.cn/). this During process, data was entered into two designated columns. The first column, for the receptor molecule, was populated with the Cas9 protein sequence in FASTA format. The second column, for the ligand molecule, was populated with the sgRNA candidate structures obtained from the molecular docking stage in PDB file format. Advanced options were available but remained unused in this study. To initiate the docking process, an email address was provided to receive the results, followed by clicking 'Submit.' The docking output included a score indicating the binding site and affinity [22]. Docking images were visualized using the Biovia Discovery Studio application (https://discover.3ds.com/).

# 2.7. Validation of optimal single guide RNA (sgRNA)

The validation stage of the optimal single guide RNA (sgRNA) candidate was performed using both cross-docking and modified cross-docking approaches. Cross-docking is a validation method that involves receptor docking with multiple native ligand variants [23]. This stage was conducted **HDOCK** using webserver http://hdock.phys.hust.edu.cn/). For cross-docking, the receptor used was the sgRNA from the complex protein with PDB ID 4ZT0, docked with the Cas9 protein. In modified cross-docking, the receptor consisted of the selected sgRNA candidate docked with the native Cas9 protein (PDB ID: 6K4S). The ligand molecules were constructed from sgRNA candidates obtained in the molecular docking stage, formatted as PDB files. Advanced options were left blank, and results were received via email following submission. The output included affinity scores and binding site data [22], with visualization

performed using the Biovia Discovery Studio application (https://discover.3ds.com/).

#### 2.8. Plasmid Construction

Plasmid construction was performed using the SnapGene application, accessible at (https://www.snapgene.com/). The plasmid used was pCMV-T7-ABE8.20m-nSpRY-P2A-EGFP (KAC1335), obtained from Benjamin Kleinstiver (Addgene plasmid #185917). The plasmid was imported into the SnapGene project, and the "Action" option was selected to choose the insertion method. The "Restriction" insertion method was

then selected, followed by choosing the fragment and inserting the sgRNA sequence. A restriction enzyme compatible with the sgRNA sequence was chosen to ensure proper fragment insertion. The cloning result was displayed on the subsequent page.

## 2.9. Dynamic Analysis

The molecular dynamics simulation was conducted using the YASARA Dynamic application (http://www.yasara.org/), developed by Bioscience GmbH (https://www.biosciencegmbh.com/).

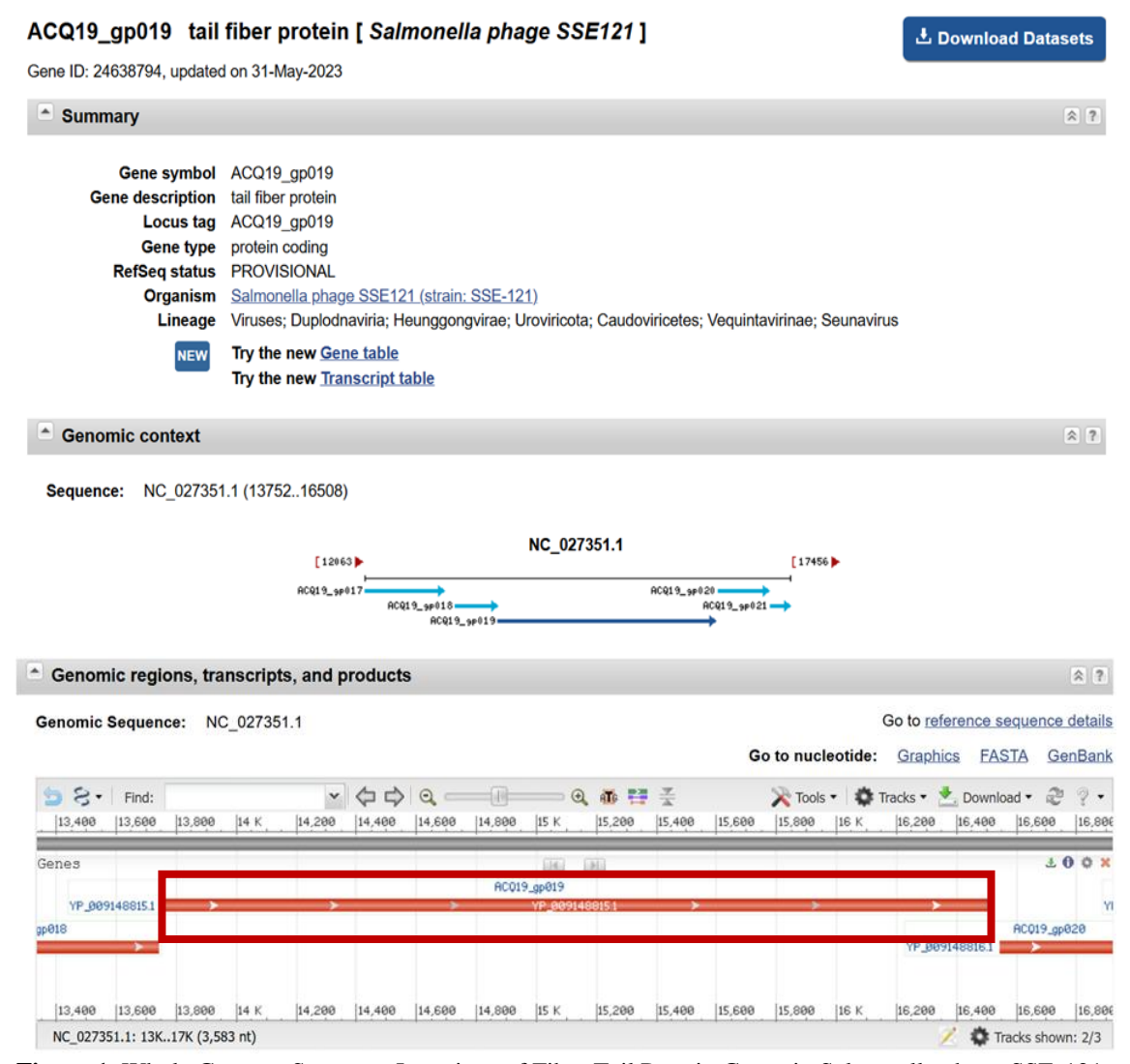


Figure 1. Whole Genome Sequence Locations of Fiber Tail Protein Genes in Salmonella phage SSE-121

The samples used in this simulation included the Cas9 protein, Cas9-sgRNA complex, and Cas9-sgRNA-DNA complex. Simulations were performed under physiological temperature and pH conditions—310K and 7.4—to mimic the in vivo

environment. The AMBER14 force field was employed due to its well-established accuracy in modeling protein-DNA interactions. Snapshots were recorded every 25 ps during the simulation to capture molecular dynamics in detail. The

Molecular Mechanics Poisson-Boltzmann Surface Area (MMPBSA) method was applied to estimate the free energy of binding, providing insights into the binding affinity and stability of the complex.

#### 3. Results and discussion

## 3.1. Sequence of sgRNA Candidate and Cas9

The complete genome, retrieved from NCBI with access number ID NC\_027351, corresponds to the Salmonella Phage SSE121. This organism possesses a variety of functional proteins, including the tail fiber protein. Tail proteins in phages are capable of recognizing bacterial host cells, penetrating their membranes, and facilitating the release of the phage genome into the host cytosol to produce new virus particles. Among these, the tail fiber protein is one of the most effective in infecting host.

The tail fiber protein is located at the distal end of the phage, making it effective in initiating binding to specific receptors on the host surface, thereby determining the infection process and host specificity [19]. The tail fiber protein analyzed in this study belongs to the Salmonella SSE-121 phage and has the locus tag ACQ19\_gp019. The sequence was retrieved from NCBI in FASTA format, corresponding to Gene ID: 24638794, and spans nucleotides 13,752 to 16,508 bp.

The Cas9 protein used in this study was obtained from the RCSB Protein Data Bank (PDB) under PDB ID 4ZT0, also in FASTA format. This protein represents the crystal structure of Streptococcus pyogenes Cas9 in complex with a single guide RNA. The FASTA file contains two distinct sequences: the upper sequence encodes the Cas9 protein, while the lower sequence corresponds to the single guide RNA. The Cas9 sequence from the FASTA file is presented in Figure 2.

>4ZTO 1|Chains A, C|CRISPR-associated endonuclease Cas9|Streptococcus pyogenes (1314) SMDKKYSIGLDIGTNSVGWAVITDDYKVPSKKFKVLGNTDRHSIKKNLIGALLFDSGETAEATRLKRT RRYTRRKNRICYLQEIFSNEMAKVDDSFFHRLEESFLVEEDKKHERHPIFGNIVDEVAYHEKYPTIYHLR KKLVDSTDKADLRLIYLALAHMIKFRGHFLIEGDLNPDNSDVDKLFIOLVOTYNOLFEENPINASGVDAK AILSARLSKSRRLENLIAQLPGEKKNGLFGNLIALSLGLTPNFKSNFDLAEDAKLQLSKDTYDDDLDNLL AQIGDQYADLFLAAKNLSDAILLSDILRVNTEITKAPLSASMIKRYDEHHQDLTLLKALVRQQLPEKYKE IFFDQSKNGYAGYIDGGASQEEFYKFIKPILEKMDGTEELLVKLNREDLLRKQRTFDNGSIPHQIHLGEL HAILRRQEDFYPFLKDNREKIEKILTFRIPYYVGPLARGNSRFAWMTRKSEETITPWNFEEVVDKGASAQ SFIERMTNFDKNLPNEKVLPKHSLLYEYFTVYNELTKVKYVTEGMRKPAFLSGEQKKAIVDLLFKTNRKV TVKOLKEDYFKKIECFDSVEISGVEDRFNASLGTYHDLLKIIKDKDFLDNEENEDILEDIVLTLTLFEDR EMIEERLKTYAHLFODKVMKQLKRRRYTGWGRLSRKLINGIRDKQSGKTILDFLKSDGFANRNFMQLIHD DSLTFKEDIOKAOVSGOGDSLHEHIANLAGSPAIKKGILOTVKVVDELVKVMGRHKPENIVIEMARENOT TOKGOKNSRERMKRIEEGIKELGSQILKEHPVENTQLQNEKLYLYYLQNGRDMYVDQELDINRLSDYDVD HIVPQSFLKDDSIDNKVLTRSDKNRGKSDNVPSEEVVKKMKNYWRQLLNAKLITQRKFDNLTKAERGGLS ELDKAGFIKRQLVETRQITKHVAQILDSRMNTKYDENDKLIREVKVITLKSKLVSDFRKDFQFYKVREIN NYHHAHDAYLNAVVGTALIKKYPKLESEFVYGDYKVYDVRKMIAKSEQEIGKATAKYFFYSNIMNFFKTE ITLANGEIRKRPLIETNGETGEIVWDKGRDFATVRKVLSMPQVNIVKKTEVQTGGFSKESILPKRNSDKL IARKKDWDPKKYGGFDSPTVAYSVLVVAKVEKGKSKKLKSVKELLGITIMERSSFEKNPIDFLEAKGYKE VKKDLIIKLPKYSLFELENGRKRMLASAGELQKGNELALPSKYVNFLYLASHYEKLKGSPEDNEQKQLFV EQHKHYLDEIIEQISEFSKRVILADANLDKVLSAYNKHRDKPIREQAENIIHLFTLTNLGAPAAFKYFDT TIDRKRYTSTKEVLDATLIHQSITGLYETRIDLSQLGGD >4ZTO\_2|Chains B, <u>D|single-quide RNA|Streptococcus</u> pyogenes (1314) GGCGCAUAAAGAUGAGACGCGUUUUAGAGCUAGAAAUAGCAAGUUAAAAUAAGCUAGUCCGUUAUCAAC

Figure 2. Cas9 Protein Sequences from PDB ID 4ZT0 file type FASTA

Single guide RNA (sgRNA) sequences were designed using the CHOPCHOP website, yielding 439 candidate sequences. The selection of sgRNA candidates was based on GC content percentage, self-complementarity, and efficiency values. Based on efficiency values, 425 sgRNA candidates were selected, each with a score above 53.65. Next, 289 sgRNA candidates were filtered, ensuring a GC content percentage above 60%. For final selection, candidates with a self-complementarity value of 0 were identified, resulting in 58 sgRNA sequences for further analysis. Data on the selected sgRNA candidates is presented in Table 1. At this stage, the selected sgRNA candidates were submitted to the

UUGAAAAAGUGUUCG

RNAcomposer website (https://rnacomposer.cs.put.poznan.pl/) to generate 3D visualizations. The inputted sequences consisted of a combination of crRNA (from CHOPCHOP results) and tracrRNA (from the 20nt Cas9 4ZT0 protein). Below is an example of the 3D visualization of an sgRNA candidate.

## 3.2. Molecular Docking sgRNA Candidate

The selection of sgRNA candidates was based on the median docking score across all data, resulting in 33 sgRNA candidates being chosen (Figure 3.). The five sgRNA candidates with the highest docking scores include: sgRNA40 (-642.88),

sgRNA27 (-631.94), sgRNA34 (-608.38), sgRNA26 (-606.7), and sgRNA52 (-604.21).

The binding results of sgRNA sequences with the target crRNA are represented in the docking score bar in Figure 4. The graph highlights the 10 sgRNA candidates with the lowest docking scores. Among the 33 sgRNA candidates that underwent docking analysis, five were selected for further evaluation. These selected candidates include sgRNA 15 (-399.18), sgRNA 11 (-372.75), sgRNA 9 (-358.67), sgRNA 57 (-352.87), and sgRNA 58 (-352.29). A lower docking score indicates lower binding energy, suggesting that the interaction is more stable [24].

## 3.3. Molecular Dynamic

Molecular dynamics analysis was conducted on several aspects, including the number of hydrogen bonds, Root Mean Square Deviation (RMSD), and Radius of Gyration (RG). The hydrogen bonds quantified through YASARA evaluation were categorized into two groups: hydrogen bonds within the solute (Figure 5.a) and hydrogen bonds between the solute and solvent (Figure 5.b). According to the analysis, an average of approximately 1,011; 1,100; and 1,125 hydrogen bonds were formed in Cas9, Cas9-sgRNA, and Cas9-sgRNA-DNA, respectively. Additionally, under solvent conditions, the number of hydrogen bonds observed was approximately 2,771 for Cas9; 3,384 for Cas9-sgRNA; and 3,559 for Cas9sgRNA-DNA.

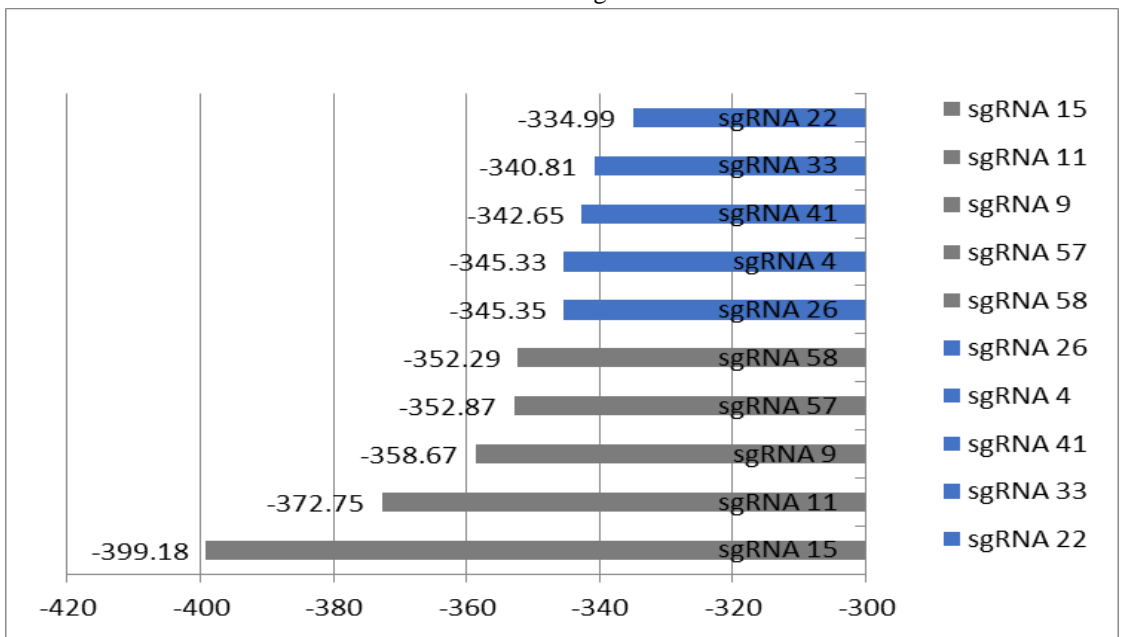
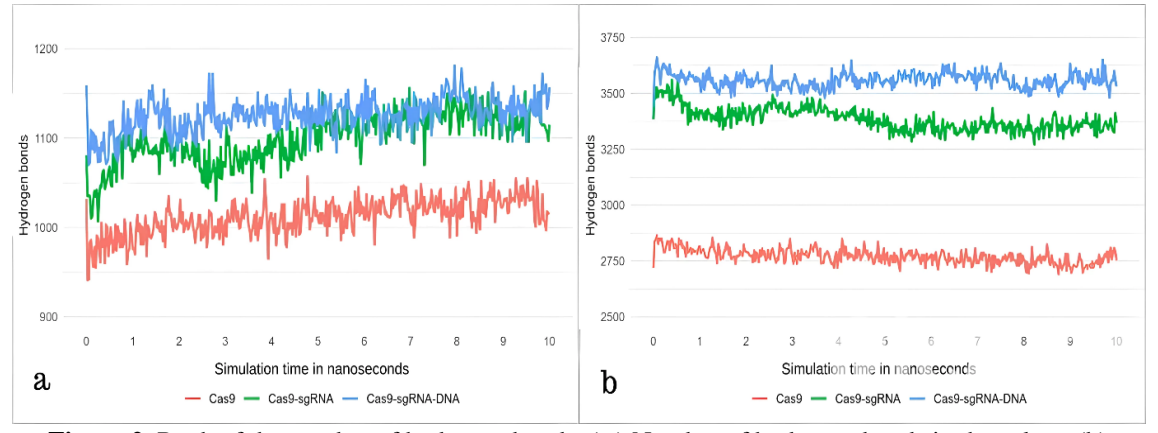
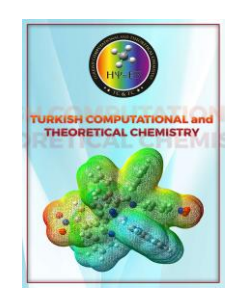


Figure 1. Graph of Cas9 Protein Docking Score of sgRNA candidate with Cas9



**Figure 2.** Raph of the number of hydrogen bonds. (a.) Number of hydrogen bonds in the solute; (b) Number of Hydrogen Bonds between Solute and Solvent.



# **Turkish Computational and Theoretical Chemistry**

Turkish Comp Theo Chem (TC&TC)

Volume(Issue): 10(1) – Year: 2026 – Pages: 165-182

e-ISSN: 2602-3237

https://doi.org/10.33435/tcandtc.1628962

**Received:** 29.01.2025 **Accepted:** 04.05.2025 Research Article



 Table 1. Selected Single Guide RNA (sgRNA) Candidates

Table 1. Selected Shigle Guide KNA (sgKNA) Candidates							
Kode	Target DNA + PAM	PAM	sgRNA Sequences	Kode	Target DNA + PAM	PAM	sgRNA Sequences
sgRNA 1	GTACCCCAGAGAAGCCCA TGCGG	CGG	GUACCCCAGAGAAGCC CAUG	sgRNA 30	TGGCAACCTGTAGGGCA AGTAGG	AGG	UGGCAACCUGUAGGG CAAGU
sgRNA 2	GAAACGCCCATTGGACCC TGTGG	TGG	GAAACGCCCAUUGGAC CCUG	sgRNA 31	CTTGTTGAAGTGACCGAC CCTGG	TGG	CUUGUUGAAGUGACC GACCC
sgRNA 3	GTCACCCATCGGTTCCCAT GCGG	CGG	GUCACCCAUCGGUUCC CAUG	sgRNA 32	CTTGTGGGCCGACATCAC CTTGG	TGG	CUUGUGGGCCGACAU CACCU
sgRNA 4	TGAATACCTTGTGGACCC TGTGG	TGG	UGAAUACCUUGUGGAC CCUG	sgRNA 33	CGCAAGCTCGAACAAAT GCTGGG	GGG	CGCAAGCUCGAACAA AUGCU
sgRNA 5	AAAGGCGATAAGGGCGAC AAGGG	GGG	AAAGGCGAUAAGGGCG ACAA	sgRNA 34	ACAGGTCCAGAAGGCCC TCAAGG	AGG	ACAGGUCCAGAAGGC CCUCA
sgRNA 6	AAGGTGATGTCGGCCCAC AAGGG	GGG	AAGGUGAUGUCGGCCC ACAA	sgRNA 35	AGCTCGAACAAATGCTG GGTGGG	GGG	AGCUCGAACAAAUGC UGGGU
sgRNA 7	AGGCCCAGAAGGTCCTGC GGGGG	GGG	AGGCCCAGAAGGUCCU GCGG	sgRNA 36	ACTGGCCCTGTCGGTCCA CAAGG	AGG	ACUGGCCCUGUCGGU CCACA
sgRNA 8	ATAGGCACAACGATCTGA GGAGG	AGG	AUAGGCACAACGAUCU GAGG	sgRNA 37	CAGCCTGACTCCAGACGT AAAGG	AGG	CAGCCUGACUCCAGAC GUAA
sgRNA 9	CGTGGAGAGAAAGGTGAC CAAGG	AGG	CGUGGAGAGAAAGGUG ACCA	sgRNA 38	CTTGGTCACCTTTCTCTC CACGG	CGG	CUUGGUCACCUUUCU CUCCA
sgRNA 10	AAGGCCCAGAAGGTCCTG CGGGG	GGG	AAGGCCCAGAAGGUCC UGCG	sgRNA 39	CAAGGTCCGAAGGGTGA TCGTGG	TGG	CAAGGUCCGAAGGGU GAUCG
sgRNA 11	AAAGGCGATAAAGGTGAC CGTGG	TGG	AAAGGCGAUAAAGGUG ACCG	sgRNA 40	GTGGCACCAGTAGCCCCT TGTGG	TGG	GUGGCACCAGUAGCC CCUUG
sgRNA 12	AAGCTCGAACAAATGCTG GGTGG	TGG	AAGCUCGAACAAAUGC UGGG	sgRNA 41	CGATCACCCTTCGGACCT TGAGG	AGG	CGAUCACCCUUCGGAC CUUG
sgRNA 13	ACAACAACAGCGGCCTTC AGCGG	CGG	ACAACAACAGCGGCCU UCAG	sgRNA 42	AAAGGCGACAAGGGTGA CACCGG	CGG	AAAGGCGACAAGGGU GACAC

# Turkish Comp Theo Chem (TC&TC), 10(1), (2026), 165-182

sgRNA 14	TAACTCCACTACTCCGCTG AAGG	AGG	UAACUCCACUACUCCG CUGA	sgRNA 43	TGTGGACCCTGTGGACCT TGTGG	TGG	UGUGGACCCUGUGGA CCUUG
sgRNA 15	CTGTGGTCGTATCTTCTGT GTGG	TGG	CUGUGGUCGUAUCUUC UGUG	sgRNA 44	TCTCCAGTTGCTGCGCCG GACGG	CGG	UCUCCAGUUGCUGCG CCGGA
sgRNA 16	GCTGAACCTATCCTTCCG GAAGG	AGG	GCUGAACCUAUCCUUC CGGA	sgRNA 45	AAAGGCGATCAGGGTGA TGAAGG	AGG	AAAGGCGAUCAGGGU GAUGA
sgRNA 17	TACTCTGGGAACTACCCG CACGG	CGG	UACUCUGGGAACUACC CGCA	sgRNA 46	GTTTCACCACGATCACCC TTCGG	CGG	GUUUCACCACGAUCA CCCUU
sgRNA 18	CGGTCCTAAAGGTGATAC TGGGG	GGG	CGGUCCUAAAGGUGAU ACUG	sgRNA 47	AAAGGTGATACTGGGGC TGATGG	TGG	AAAGGUGAUACUGGG GCUGA
sgRNA 19	AGAGGGTCAGATGGGTGC TGGGG	GGG	AGAGGGUCAGAUGGGU GCUG	sgRNA 48	GTGACCGACCCTGGTGA AGAAGG	AGG	GUGACCGACCCUGGU GAAGA
sgRNA 20	AAGACCTTCTTCACCAGG GTCGG	CGG	AAGACCUUCUUCACCA GGGU	sgRNA 49	AAGGGCGACAAGGGTGA TCAAGG	AGG	AAGGGCGACAAGGGU GAUCA
sgRNA 21	CTACCGCATGGGCTTCTCT GGGG	GGG	CUACCGCAUGGGCUUC UCUG	sgRNA 50	ACAACTGGGGCTATGGA TGTTGG	TGG	ACAACUGGGGCUAUG GAUGU
sgRNA 22	CAGCAGGAGGAAGTTGGG ATGGG	GGG	CAGCAGGAGGAAGUUG GGAU	sgRNA 51	TACTGGCGGTGGAACCTT TGTGG	TGG	UACUGGCGGUGGAAC CUUUG
sgRNA 23	TCTACTGGAGAGCTTGGT CAGGG	GGG	UCUACUGGAGAGCUUG GUCA	sgRNA 52	CTTCCTTCTACTGGAGAG CTTGG	TGG	CUUCCUUCUACUGGA GAGCU
sgRNA 24	CAAGGTCCACAGGGTCCA CAAGG	AGG	CAAGGUCCACAGGGUC CACA	sgRNA 53	GGTGCTGGGGTAGAAAT CCTTGG	TGG	GGUGCUGGGGUAGAA AUCCU
sgRNA 25	ACTGGTTTAACTGGCCCT GTCGG	CGG	ACUGGUUUAACUGGCC CUGU	sgRNA 54	TGGTTGCAGCAGGAGGA AGTTGG	TGG	UGGUUGCAGCAGGAG GAAGU
sgRNA 26	ACCGGGGCTACAGGGGAT GTCGG	CGG	ACCGGGGCUACAGGGG AUGU	sgRNA 55	TCTCTGGGGTACATGGGT GGAGG	AGG	UCUCUGGGGUACAUG GGUGG
sgRNA 27	CCAAGGCCCAGAAGGTCC TGCGG	CGG	CCAAGGCCCAGAAGGU CCUG	sgRNA 56	GACCAGATGTGGGTTTG GACTGG	TGG	GACCAGAUGUGGGUU UGGAC
sgRNA 28	GCAGTCAGTGAAACGCCC ATTGG	TGG	GCAGUCAGUGAAACGC CCAU	sgRNA 57	GTAGCACCTGCGGGACC TTGAGG	AGG	GUAGCACCUGCGGGA CCUUG
sgRNA 29	AAAAGGCGATAAGGGCG ACAAGG	AGG	AAAAGGCGAUAAGGGC GACA	sgRNA 58	AGCGGCCTTCAGCGGAG TAGTGG	TGG	AGCGGCCUUCAGCGG AGUAG

# Turkish Comp Theo Chem (TC&TC), 10(1), (2026), 165-182

<b>Table 2</b> . 3D Visualization of Single Guide RNA (sgRNA 1)						
Kode	Visualization 3D sgRNA	sgRNA sequences				
sgRNA 1	A THE WAY	GUACCCCAGAGAAGCCCAUGGUUUUAG AGCUAGAAAUAGCAAGUUAAAAUAAGG CUAGUCCGUUAUCAACUUGAAAAAGUG UUCG((((((((())))))))).(.((().)).)				

## **Turkish Computational and Theoretical Chemistry**

Turkish Comp Theo Chem (TC&TC)



e-ISSN: 2602-3237

https://doi.org/10.33435/tcandtc.1628962

**Received:** 29.01.2025 Accepted: 04.05.2025 Research Article

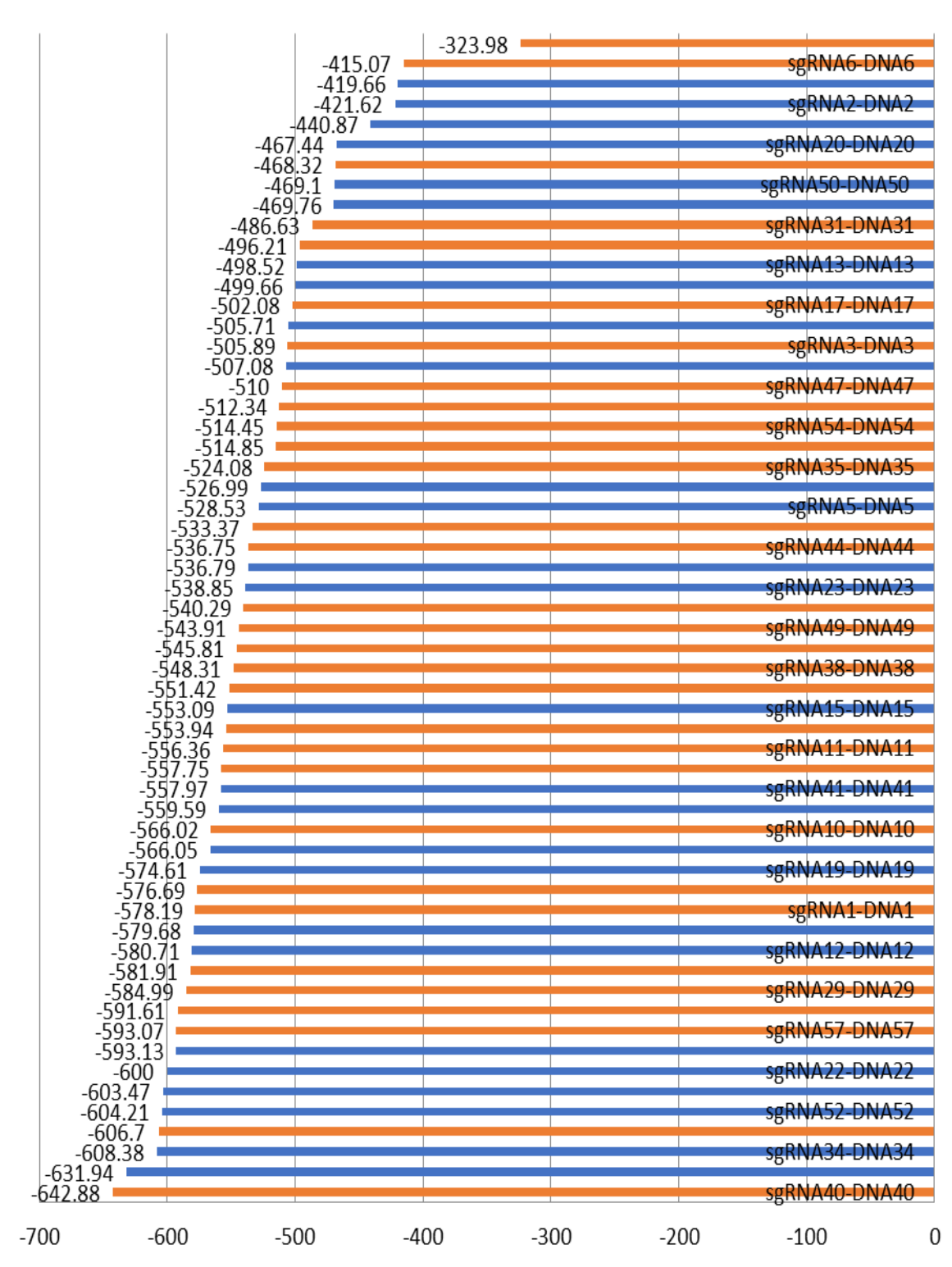
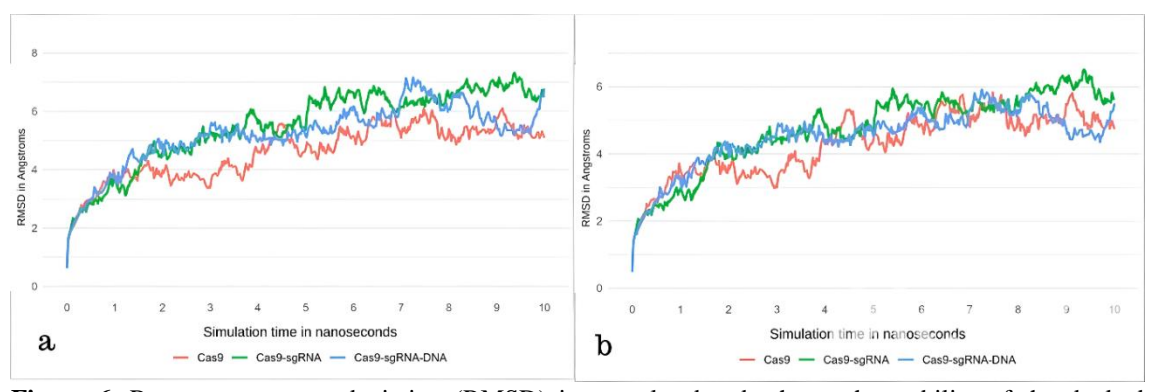


Figure 3. Graph of Docking Score sgRNA with crRNA Target



**Figure 6**. Root mean square deviation (RMSD) in complex bonds shows the stability of the docked complex. (a) Total RMSD on Cas9, Cas9-sgRNA, and Cas9-sgRNA-DNA, (b)  $C\alpha$  RMSD on Cas9, Cas9-sgRNA, and Cas9-sgRNA-DNA

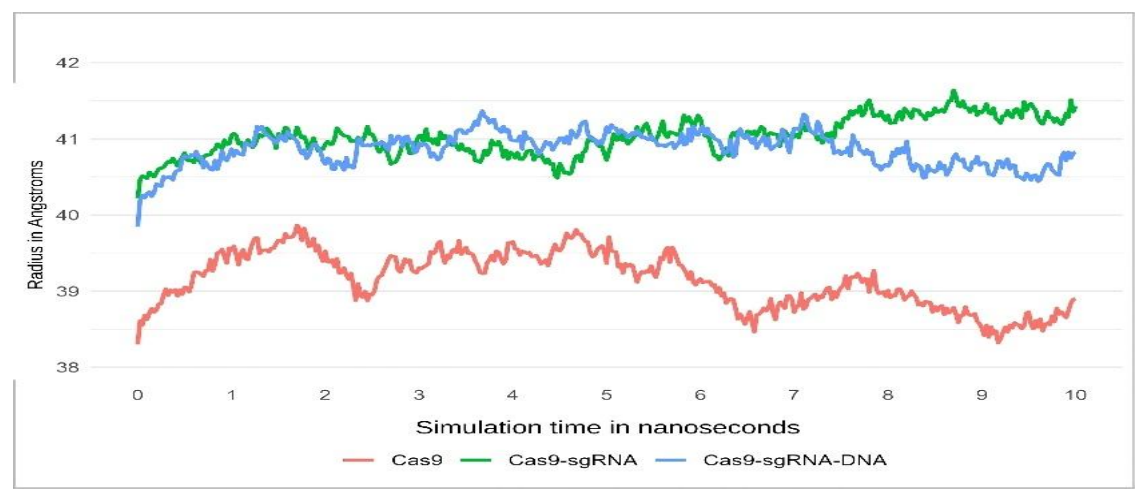
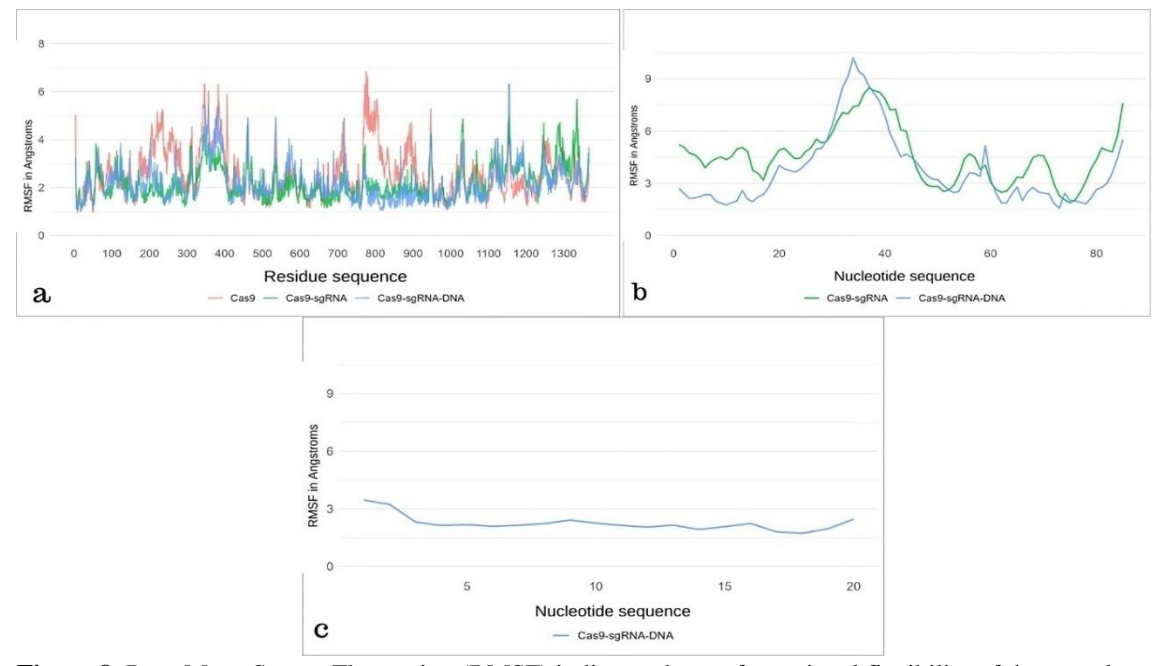


Figure 3. Comparison of RG patterns between single Cas 9 protein and Cas 9-sgRNA complexes



**Figure 8**. Root Mean Square Fluctuation (RMSF) indicates the conformational flexibility of the complex. (a.) RMSF of Cas9 amino acid residues in single and complex samples, (b.) RMSF of sgRNA structure nucleotides in complex samples, (c.) RMSF of DNA in Cas9-sgRNA-DNA complex sample.

Based on the average RMSD values, the Cas9, Cas9-sgRNA complex, and Cas9-sgRNA-DNA complex exhibited deviations of 4.606 Å, 5.512 Å, and 5.212 Å, respectively (Figure 6.a). This suggests a substantial conformational change from the initial structure. Additionally, the lower RMSD values of C-alpha for all three samples—averaging 4.305 Å, 4.752 Å, and 4.503 Å, respectively (Figure 6.b)—indicate that the protein core remained relatively stable despite extensive structural changes.

Radius of gyration (Rg) is a parameter that describes the equilibrium conformation and mass distribution of a molecule during simulation. A lower Rg value signifies a compact or folded

protein structure, while higher values indicate a more open or unfolded state. The Rg graph (Figure 7) illustrates the structural changes of Cas9, Cas9sgRNA, and Cas9-sgRNA-DNA over the course of the 10-nanosecond simulation. Cas9 exhibits a lower Rg value with a decreasing trend over time, suggesting that its structure becomes more compact as the simulation progresses. In contrast, the Cas9and Cas9-sgRNA-DNA complexes, sgRNA represented by green and blue lines, display higher Rg values than pure Cas9. This indicates that the incorporation of sgRNA and DNA increases the overall molecular size, potentially due to the more open conformation required to accommodate the additional components.

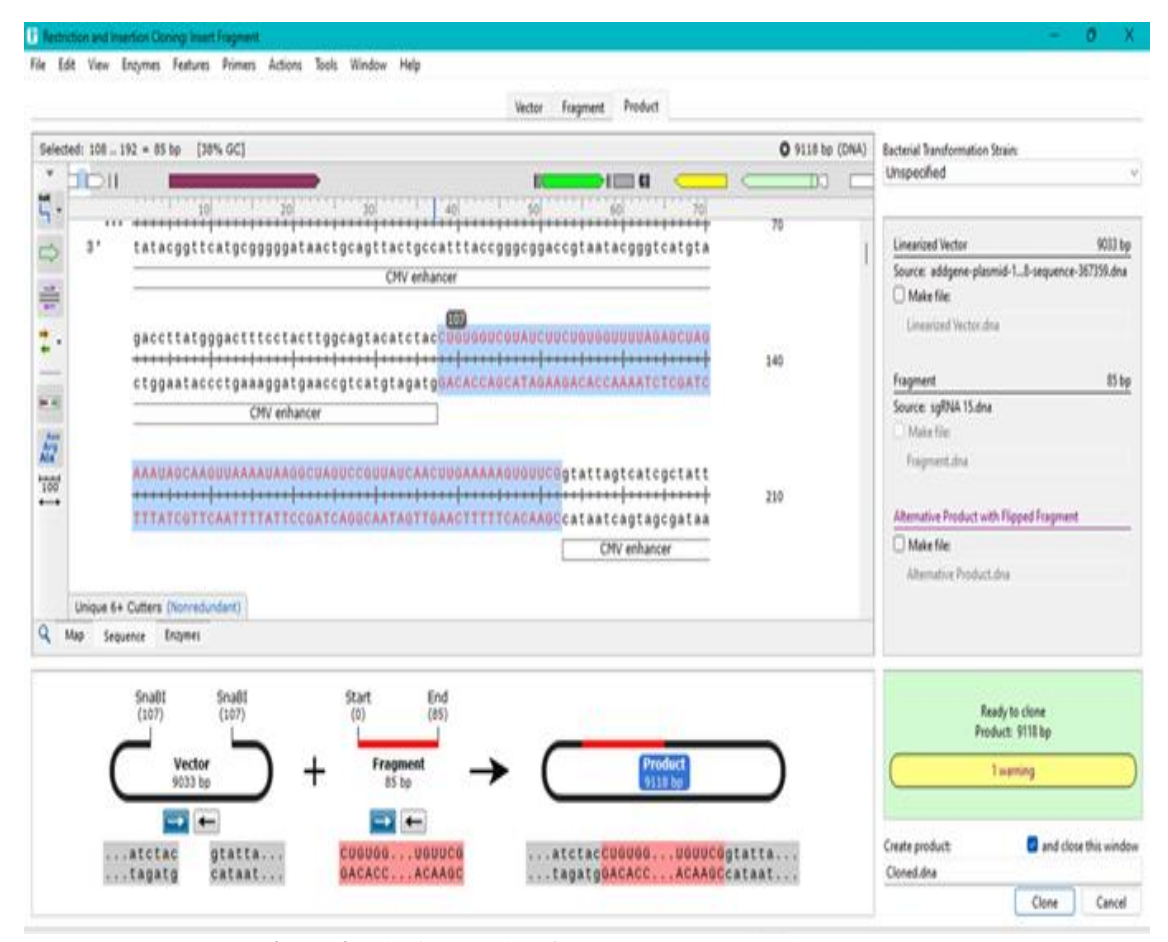


Figure 9. Cloning results of pCMV-T7-ABE8 and sgRNA 15

The RMSF graph in Figure 8 illustrates the flexibility profile of Cas9 residues and their complexes with sgRNA and DNA. Pure Cas9, represented by the red line, exhibits greater fluctuations compared to the Cas9-sgRNA and

Cas9-sgRNA-DNA complexes. The RMSF graphs for sgRNA within the Cas9-sgRNA and Cas9-sgRNA-DNA complexes (Figure 8.b) display nearly identical patterns, suggesting that the presence of DNA does not significantly alter the

flexibility of the sgRNA backbone. Both graphs exhibit consistent peaks and valleys, indicating that specific nucleotides in the sgRNA maintain similar mobility or rigidity, regardless of the presence of target DNA. Meanwhile, the RMSF graph for the Cas9-sgRNA-DNA complex (Figure 8c) presents a relatively stable and low fluctuation profile along the nucleotide sequence, indicating that the DNA within this complex maintains consistent structural rigidity.

#### 3.4. Plasmid Construct

In-silico plasmid construction aims to map recognition sites for target sequences and appropriate restriction enzymes before implementation in in vitro studies. The plasmid used in this study features a T7 promoter site and a Cas9 protein site for DNA cleavage [25]. The constructed single guide RNA (sgRNA 15) was inserted into the pCMV-T7-ABE8 plasmid to direct the Cas9 protein toward the specific target genome region for cleavage. The pCMV-T7-ABE8 plasmid and sgRNA 15 were digested using the restriction enzyme SnaBI and subsequently ligated to form a recombinant plasmid. The successful insertion of the gene into the plasmid is confirmed by the preservation of the reading frame, ensuring proper protein expression [26]. The well-ligated sgRNA 15 sequences within the pCMV-T7-ABE8 plasmid was visualized using SnapGene, as illustrated in Figure 9.

## 4. Conclusions

Salmonella enterica has been a significant public health concern, primarily as a cause of foodborne illnesses, for more than a century. Due to its abundance and high infection rates, researchers have continuously sought effective treatment options [27]. One of the most commonly used treatments is antibiotics. However, this approach has become less effective due to the ability of bacteria to develop antibiotic resistance. Multiple studies have demonstrated the high level of resistance in multi-drug-resistant Salmonella spp., highlighting the consequences of uncontrolled antibiotic use and its impact on the diminished effectiveness of combating Salmonella infections[28], [29], [30]. As an alternative, bacteriophage therapy has been explored for Salmonella treatment. Unlike antibiotics, which exhibit broad-spectrum activity, bacteriophages are highly host-specific, reducing the risk of intestinal dysbiosis and secondary infections following phage therapy [31]. To expand the host range of bacteriophages, genome editing presents a viable strategy. Bacteriophages contain tail fiber proteins, which play a crucial role in the infection process by interacting with receptors on the bacterial host surface. These tail fiber proteins contain receptorbinding domains that determine host specificity. Thus, editing these regions has the potential to enhance the host range [32]. The in-silico construction of sgRNA as part of the CRISPR-Cas system has previously been performed on the tail fiber protein Gp0047 of Salmonella Phage SSE-121 [33]. In that study, candidate sgRNA 6 was identified, demonstrating stable interactions with the Cas9 protein [33]. In contrast, the present study focuses on the gp19 tail fiber protein of Salmonella Phage SSE-121 as the primary target for enabling specific recognition of bacterial host cells.

The construction of single guide RNA in Salmonella phage in silico aims to obtain optimal candidates that will later be used in in vitro studies. The Salmonella phage SSE-121 genome was inserted into the CHOPCHOP website, and 493 data were generated based on the off-target score. CHOPCHOP helps simplify the design of sgRNA used in CRISPR. The application of this website is generally used to create knock-out genes through the introduction of double-strand breaks followed by repair through the NHEJ pathway [34]. The results obtained were then selected based on the efficiency score, GC content, and selfcomplementary. The efficiency score in this study was obtained based on the median results of all data obtained from the CHOPCHOP website. The median of the data obtained is 52.6. GC content is the percentage of nucleotide bases containing guanine and cytosine bases in a DNA sequence. The data obtained has GC content between 50%-70%. Self-complementary is the value of the ability of a DNA fragment to bind to itself. This value is important in a selection of sgRNA candidates where the optimal candidate used has a selfcomplementary value of 0, so 58 sgRNA candidates were selected from all candidate data obtained. Selected sgRNA candidates were docked with target DNA to evaluate their binding ability. Each sgRNA candidate consists of crRNA and tracrRNA, which are essential for molecular docking. The crRNA is responsible for recognizing and targeting invading nucleic acids, while the tracrRNA binds to the crRNA to facilitate its maturation and enable subsequent interference by Cas9. This combination allows the sgRNA to guide the Cas9 protein in cleaving the desired DNA strand [13], [35]. As a result, 33 sgRNA candidates with low docking scores were identified. The next phase

involved docking these sgRNA candidates with

Cas9 protein sequences. Molecular docking between sgRNA and Cas9 protein was performed using HNADock, a tool designed to model the structural complexes formed between nucleic acids. HNADock utilizes an FFT-based global docking algorithm to evaluate binding interactions and applies an intrinsic scoring function RNA/DNA-RNA/DNA interactions. This scoring function incorporates distance-dependent calculations, where the receptor lattice points and surrounding lattices contribute to the overall binding energy score [36]. Molecular docking for single guide RNA (sgRNA) follows a distinct approach compared to traditional docking methods used in drug development, which involve complex molecules such as carbohydrates, lipids, or peptides. For complex molecules, the docking process requires multiple preparation steps, including protein modeling, ligand molecule optimization, and molecular calculations. The preparation steps and methodologies employed in software such as AutoDock Vina differ from those used in HNADock and HDOCK [32], [37].

Following the identification of 33 candidates, an additional selection process was conducted, narrowing the list to five sgRNA candidates with the lowest docking scores. A lower docking score indicates lower binding energy, suggesting increased stability of the interaction. The receptor and ligand molecules processed through the HDOCK software were analyzed using a hybrid algorithm that combines both template-based and template-free docking approaches to predict molecular interactions [22]. The final selected candidate, sgRNA 15, exhibited a docking score of -553.09 for target DNA binding and -399.18 for its interaction with the Cas9 protein.

Molecular Dynamics (MD) simulations have been an excellent complement to experimental studies that investigate the CRISPR/Cas9 mechanism in terms of structure, thermodynamics, and kinetics [38]. The binding of sgRNA is one of the important steps in CRISPR/Cas9 activity because sgRNA guides the Cas9 nuclease to bind to the target DNA. A study conducted by Palermo et al. in 2017 using Gaussian Accelerated Molecular Dynamics (GaMD) and targeted Molecular Dynamics (tMD) to show the conformational changes of Cas9 in response to sgRNA binding in atomic detail [39]. The hydrogen bonds formed between the ligand and the protein are responsible for maintaining a compact and appropriately oriented structure, where the flexibility of the protein residues also comes into play, as it is these compounds that form bonds with the ligand molecules [40]. The number of hydrogen bonds generated from the YASARA evaluation falls into two categories, namely, the number of hydrogen bonds within the solute (Fig5.a) and the number of hydrogen bonds between the solute and solvent (Fig5.b). The protein folding process is indicated by the increasing trend of the number of hydrogen bonds in the solute (Fig5.a) and the decreasing number of hydrogen bonds between the solute and solvent (Fig5.b). The patterns observed in both graphs confirmed that Cas9 and Cas9-sgRNA underwent protein folding optimization throughout the simulation, while the Cas9-sgRNA-DNA complex underwent conformational stability, with a trend of a relatively constant number of hydrogen bonds throughout the simulation.

RMSD is a key parameter in structural analysis that measures the conformational changes of receptor macromolecules in response to interactions with ligands. The RMSD measures the extent to which the receptor changes from its initial conformation, providing an indicator of the structural stability during the simulation. This dynamic stability is important as sustained conformational changes may reflect folding, unfolding, or bonding events [41]. The RMSD value considered standard for protein stability during simulation is less than 3 Å. If the RMSD value of a protein exceeds this threshold, it can be interpreted that the protein has undergone significant conformational changes due to folding. unfolding, or binding events. The average RMSD values for Cas9, Cas9-sgRNA complex, and Cas9sgRNA-DNA complex in Figure 6 (a,b) show substantial conformational changes from the initial structure. In contrast to the lower RMSD values of C-alpha for the three samples, as in Figure 7(a,b), each graph indicates that the protein core remains relatively stable despite extensive changes to the overall structure. High RMSD graphs may also imply major conformational transitions occurring in the protein to obtain a stable conformation with the ligand [40]. The changes that occur are predicted to be significant and do not automatically indicate protein malfunction. Instead, in many cases, they may reflect structural adjustments required for functional interaction with the ligand or target DNA in the context of the genome editing mechanism by the CRISPR-Cas9 system.

Another parameter is the radius of gyration (Rg), which is considered a fundamental indicator of the total size of the chain molecules. Rg is a parameter that describes the equilibrium conformation and mass distribution of a molecule in the simulation. A low Rg indicates a compact or folded protein conformation, while higher values indicate an open or unfolded state [42]. The Rg graph (Figure 8) shows records of the structural changes of Cas9, Cas9-sgRNA, and Cas9-sgRNA-DNA throughout the 10-nanosecond simulation. Cas9 shows a lower Rg value and a decreasing trend over time, indicating a structure that becomes more compact

as the simulation progresses. This indicates a stable and well-folded conformation, which is important for protein function in its natural state. The Cas9sgRNA and Cas9-sgRNA-DNA complexes, shown with green and blue lines, exhibit higher Rg values than pure Cas9, indicating that the presence of sgRNA and DNA increases the overall size of the complex, possibly due to the more open structure required to accommodate the additional molecules. However, the relatively stable Rg values for both complexes indicate that despite the structural expansion, the complexes still achieve specific conformational stability throughout the simulation. This could imply that Cas9 in complex with sgRNA and DNA retains a sufficiently defined structure to perform its function of target DNA recognition and cutting, with the stability required for efficient genome editing activity [43].

RMSF measures the local flexibility of the protein structure by assessing the deviation of specific atoms or residues throughout the simulation. Variations in flexibility in terms of RMSF parameters can be used to investigate the binding of inhibitors to the target. The RMSF plot will be a typical representation of residues that undergo significant changes during MD simulation operation [42]. Low RMSF values indicate rigid and stable regions of the protein, which are often associated with core structural elements or functionally important regions. On the other hand, high RMSF values signify regions with more flexibility, which may play a role in protein interactions, conformational changes, or regions exposed to solvents. The graph of Figure 8. indicates that Cas9 in its pure form has higher flexibility at some of its residues, which may reflect the need for the protein's natural structure to adapt or change conformation in its search and binding of target DNA. Meanwhile, Cas9-sgRNA and Cas9sgRNA-DNA complexes appear to have lower RMSF profiles overall, suggesting that binding to sgRNA and DNA might stabilize the protein structure and reduce its flexibility. This is consistent with the suggestion that complexation with sgRNA and DNA guides the protein into a more ordered and specific conformation required for effective gene editing activity.

The RMSF graphs for sgRNA in Cas9-sgRNA and Cas9-sgRNA-DNA complexes in Figure 8.b show consistency that reflects the innate structural constraints of sgRNA when bound to Cas9, which are retained after DNA binding, ensuring that sgRNA remains in the correct conformation required to direct Cas9 to the target DNA site. Slight variations between the two complexes may represent subtle adjustments to the sgRNA conformation in response to DNA binding, which is essential for the formation of the active Cas9-

sgRNA-DNA complex required for gene editing. The RMSF graph for the Cas9-sgRNA-DNA complex in Figure 8.c shows a relatively stable and low profile along the nucleotide sequence, indicating that the DNA in this complex has consistent rigidity. The absence of significant peaks indicates that not many DNA residues experience high flexibility, which could indicate that the DNA is stably bound by the Cas9-sgRNA complex and does not undergo much conformational change during the simulation. This stability is important for maintaining the integrity of the interaction between Cas9, sgRNA, and target DNA, which is crucial for precision in the recognition and cutting of DNA target sites by the CRISPR-Cas9 system.

The results of the sgRNA construction were then used to reconstruct the plasmid. Plasmid construction uses a T7 promoter to regulate gene expression in recombinant bacteriophage proteins. The plasmid used is the pCMV-T7-ABE8, which is equipped with a T7 promoter and Cas9 protein. sgRNA 15 cuts the plasmid using the SnaBI restriction enzyme located at sequence number 107. The cutting region is recommended to be in the direction before the T7 sequence and Cas9 protein so that the expression process can work properly. Plasmids inserted by sgRNA sequences will be visualized in the Snapgene application as plasmid cloning.

The in-silico construction of sgRNA enabled the identification of an optimal candidate for genome editing in Salmonella phage SSE-121 using various computational tools. The selected sgRNA candidate, which exhibited the lowest docking score, was incorporated into plasmid construction. Hydrogen bond formation was analyzed across different molecular complexes, with averages of approximately 1,011 in Cas9; 1,100 in Cas9sgRNA; and 1,125 in Cas9-sgRNA-DNA. Under solvent conditions, the number of hydrogen bonds increased to approximately 2,771 for Cas9; 3,384 for Cas9-sgRNA; and 3,559 for Cas9-sgRNA-DNA. The average RMSD values for Cas9, Cas9sgRNA, and Cas9-sgRNA-DNA complexes suggested substantial conformational changes from the initial structure. However, the RMSD values of C-alpha remained lower across all three samples, indicating that the protein core retained relative stability despite extensive structural modifications. Cas9 exhibited lower Rg values with a decreasing trend over time, reflecting an increasingly compact structure throughout the simulation. Additionally, the lower RMSF profiles of Cas9-sgRNA and Cas9-sgRNA-DNA suggest that sgRNA and DNA binding contributed to structural stabilization and reduced flexibility. The pCMV-T7-ABE8 plasmid was successfully modified by integrating the sgRNA15 sequence using the SnaBI restriction

enzyme for plasmid cloning. These recombinant plasmids will be utilized in subsequent in vivo and in vitro studies to advance genome editing applications

## ACKNOWLEDGEMENT

This work was part of research supported by BRIN through RIIM grant with contract number 3759/UN25.3.1/LT/2023 under the name of Erlia Narulita. The content is solely the responsibility of the authors and does not necessarily represent the official views of the Institution.

## References

- [1] Y He, J Wang, R Zhang, L Chen, H Zhang, X Qi, J Chen, Epidemiology of foodborne diseases caused by Salmonella in Zhejiang Province, China, between 2010 and 2021. Front. Public Heal. 11 (2023) 1–10.
- [2] M Pal, T Ragasa, T R Abdeta, R Zende, Salmonellosis Remains the Hidden Menace in Our Global Food Supply: A Salmonellosis Remains the Hidden Menace in Our Global Food Supply: A Comprehensive Review. Am [12] J Med Biol Res 12(1) (2024) 1–12.
- [3] O Ehuwa, A K Jaiswal, S Jaiswal, Salmonella, food safety and food handling practices. Foods 10 (5) (2021) 1–16.
- [4] M M S Dallal, A Nasser, S Karimaei, Characterization of Virulence Genotypes, Antimicrobial Resistance Patterns, and Biofilm Synthesis in Salmonella spp Isolated from Foodborne Outbreaks. Can J Infect Dis Med Microbiol (2024).
- [5] R E Castro-Vargas, M P Herrera-Sánchez, R Rodríguez-Hernández, I S Rondón-Barragán, Antibiotic resistance in Salmonella spp. isolated from poultry: A global overview. Vet World 13(10) (2020) 2070–2084.
- [6] L K Francois Watkins, S Luna, B B Bruce, F Medalla, J L Reynolds, L C Ray, E L Wilson, H Caidi, P M. Griffin, Clinical Outcomes of Patients With Nontyphoidal Salmonella Infections by Isolate Resistance—Foodborne Diseases Active Surveillance Network, 10 US Sites, 2004–2018. Clin Infect Dis 78(3) (2024) 535–543.
- [7] H H Hadimli, S Aslı, G S Gölen, Evaluation [17] of the effectiveness of bacteriophage therapy against Salmonella infections in mice. Eurasian J Vet Sci 37 (2022) 83–89.

- [8] H. Bao, Y Zhoua, K Shahin, H Zhang, F Cao, M Pang, X Zhang, S Zhu, A Olaniran, S Schmidt, R Wang, The complete genome of lytic Salmonella phage vB\_SenM-PA13076 and therapeutic potency in the treatment of lethal Salmonella Enteritidis infections in mice. Microbiol Res 237 (2020).
- [9] E Koç, S Yetişkin, A Yücefaydali, D Tunalier, Y Soyer, Effect of egg cultivation methods on Salmonella prevalence and the promising prevention strategy: bacteriophage therapy. Food Sci Biotechnol 2025.
- [10] L. Bianchessi, G. De Bernardi, M. Vigorelli, P. Dall'Ara, L. Turin, Bacteriophage Therapy in Companion and Farm Animals. Antibiotics 13(4) (2024).
- [11] S. Liang, Y. Qi, H. Yu, W. Sun, S. H. A. Raza, S. S. Alkhalil, E. E. A. Salama, L. Zhang, N. Alkhorayef, Bacteriophage Therapy as an Application for Bacterial Infection in China. Antibiotics 12(2) (2023) 1–20.
- [12] M. L. Zhang, H. Bin Li, Y. Jin, Application and perspective of CRISPR/Cas9 genome editing technology in human diseases modeling and gene therapy. Front Genet 15 (2024) 1–14.
- [13] M. A. Mengstie, M. T. Azezew, T. A. Dejenie, A. A. Teshome, F. T. Admasu, A. B. Teklemariam, A. T. Mulu, M. M. Agidew, D. G. Adugna, H. Geremew, E. C. Abebe, Recent Advancements in Reducing the Off-Target Effect of CRISPR-Cas9 Genome Editing. Biol Targets Ther 18 (2024) 21–28.
- [14] A. Bao, D. J. Burritt, H. Chen, X. Zhou, D. Cao, L. S. P. Tran, The CRISPR/Cas9 system and its applications in crop genome editing. Crit Rev Biotechnol 39(3) (2019) 321–336.
- [15] A. Rácz, L. M. Mihalovits, D. Bajusz, K. Héberger, R. A. Miranda-Quintana, Molecular Dynamics Simulations and Diversity Selection by Extended Continuous Similarity Indices. J Chem Inf Model 62(14) (2022) 3415–3425.
- [16] F Jiang, K Zhou, L Ma, S Gressel, J A Doudna, A Cas9-guide RNA complex preorganized for target DNA recognition. Science 348 (2015) 1477–1481.
- I. Halim, M. H. Fendiyanto, Miftahudin, SgRNA design for DLT gene editing using CRISPR-Cas9 and in-silico mutation prediction in Rice cv. Hawara Bunar. IOP Conf Ser Earth Environ Sci 948 (1) 2021.

- [18] K. Labun, T. G. Montague, M. Krause, Y. N. Torres Cleuren, H. Tjeldnes, E. Valen, CHOPCHOP v3: Expanding the CRISPR web [28] toolbox beyond genome editing. Nucleic Acids Res 47 (2019) 171–174.
- [19] M. Antczak, M. Popenda, T. Zok, J. Sarzynska, T. Ratajczak, K Tomczyk, R.W. Adamiak, M. Szachniuk, New functionality of RNAComposer: An application to shape the [29] axis of miR160 precursor structure. Acta Biochim Pol 63 (2016) 737–744.
- [20] I. P. Maksum, A. F. Maulana, M. Yusuf, R. Mulyani, W. Destiarani, R. Rustaman, [30] Molecular Dynamics Simulation of a tRNA-Leucine Dimer with an A3243G Heteroplasmy Mutation in Human Mitochondria Using a Secondary Structure Prediction Approach. Indones J Chem 22 (2022) 1043–1051.
- [21] S. Sartaj Sohrab, S. Aly El-Kafrawy, E. Ibraheem Azhar, In silico prediction and experimental evaluation of potential siRNAs [31] against SARS-CoV-2 inhibition in Vero E6 cells. J King Saud Univ Sci 34 (2022) 1–8.
- [22] Y. Yan, H. Tao, J. He, S. Y. Huang, The [32] HDOCK server for integrated protein–protein docking. Nat Protoc 15 (2020) 1829–1852.
- [23] E. Mateev, I. Valkova, B. Angelov, M. Georgieva, A. Zlatkov, Validation Through Re-Docking, Cross-Docking and Ligand Enrichment in Various Well-Resoluted Mao-B Receptors. Int J Pharm Sci Res 13 (2022) [33] 1099–1107.
- [24] X. Du, Y. Li, Y. L. Xia, S. M. Ai, J. Liang, P. Sang, X. L. Ji, S. Q. Liu, Insights into protein—ligand interactions: Mechanisms, models, and methods. Int J Mol Sci 17 (2016) 1–34.
- [25] M. Oktavioni, D. H. Tjong, J. Jamsari, In-silico construction of potential cis-acting elements from PD\_CbNPR1 with T7 minimal promoter. IOP Conf Ser Earth Environ Sci 741 (2021) 1– [35] 8.
- [26] N. A. Setiani, U. Baroroh, A. P. Handayani, N. Chairunnisa, I. Mardiah, Konstruksi Plasmid Rekombinan pET-28a-Nanobodi Secara In Silico. 2 (2022) 256–264.
- [27] O. Oludairo, J. K. P. Kwaga, J. Kabir, P. A. Abdu, A. Gitanjali, A. Perrets, V. Cibin, A. A. Lettini, J. O. Aiyedun, Review of Salmonella Characteristics, History, Taxonomy, Nomenclature, Non Typhoidal Salmonellosis

- (NTS) and Typhoidal Salmonellosis (TS). Zagazig Vet J 50 (2022) 160–171.
- J Pławińska-czarnak, K Wódz, M Kizerwetter-'Swida, J Bogdan, P Kwieci 'nski, T Nowak, Z Strzałkowska, K Anusz. Multi-Drug Resistance to Salmonella spp. When Isolated from Raw Meat Products. Antibiotics 11 (2022) 1–13.
- 9] S Wu, J P Hulme, Recent advances in the detection of antibiotic and multi-drug resistant Salmonella: An update. Int J Mol Sci 22 (2021).
- M T Mumbo, E N Nyaboga, J K Kinyua, E K Muge, S G K Mathenge, H Rotich, G Muriira, B Njiraini, J M Njiru, Antimicrobial resistance profiles of Salmonella spp. and Escherichia coli isolated from fresh nile tilapia (Oreochromis niloticus) fish marketed for human consumption. BMC Microbiol 23 (2023) 1–18.
- M. A. S. Khan, S. R. Rahman, Use of Phages to Treat Antimicrobial-Resistant Salmonella Infections in Poultry. Vet Sci 9 (2022) 1–20.
- N. Akter, S Saha, Md. A Hossain, K M Uddin, A R Bhat, S Ahmed, S M A Kawsar, Acylated glucopyranosides: FTIR, NMR, FMO, MEP, molecular docking, dynamics simulation, ADMET and antimicrobial activity against bacterial and fungal pathogens. Chem. Phys. Impact 9 (2024).
- Narulita, A N Oktarina, R B Opulencia, A H Widianto, R A Febrianti, H S Addy, CRISPR-Cas Single-Guide RNA Construction for Tail Fiber Gene Gp0047 of Salmonella. Turkish Comp Theo Chem 9 (2025) 25–37.
- [34] K. Labun, M. Krause, Y. T. Cleuren, E. Valen, CRISPR Genome Editing Made Easy Through the CHOPCHOP Website. Current Protocol 1 (2021) 1–19.
  - L. Sakovina, I Vokhtantsev, E Akhmetova, M Vorobyeva, D O Zharkov, D Novopashina, P Vorobjev, Photocleavable Guide crRNAs for a Light-Controllable CRISPR / Cas9 System. Int J Mol Sci 25 (2024) 1–13.
- [36] J. He, J. Wang, H. Tao, Y. Xiao, S. Y. Huang, HNADOCK: a nucleic acid docking server for modeling RNA/DNA-RNA/DNA 3D complex structures. Nucleic Acids Res 47 (2019) 35– 42.

- [37] I. I. Arabi, Md A Hossain, S M A Kawsar, N Joshi, J M Kalra, N Gairola, J Suyal, A Semwal, R Zainul, V Jakhmola, S Saha, Glucopyranoside Derivatives as Antibacterial and Antifungal Agents: QSAR, Molecular Docking and ADMET Analyses. Adv. J. Chem. Sect. A 7 (2024) 758–776.
- [38] M. Yang, Molecular dynamics simulations: Chemical advances and applications. J Phys Conf Ser 2608 (2023) 4–6.
- [39] S. Bhattacharya, P. Satpati, Insights into the Mechanism of CRISPR / Cas9-Based Genome Editing from Molecular Dynamics Simulations. ACS Omega 8 (2023) 1817-1837.
- [40] J Sharma, V Kumar, R Singh, V Rajendran, An in-silico evaluation of different bioactive molecules of tea for their inhibition potency against non structural protein-15 of SARS-CoV-2. Food Chem 346 (2020) 1–8.
- [41] A. Mangin, V. Dion, G. Menzies, Developing small Cas9 hybrids using molecular modeling. Sci Rep 14 (2023) 1–31.
- [42] S Ghahremanian, M Mehdi, K Raeisi, D Toghraie, Molecular dynamics simulation approach for discovering potential inhibitors against SARS-CoV-2: A structural review. J Mol Liq 354 (2020) 1–12.
- [43] M Borjian, M Shahbazi, M Shokrgozar, H Rahimi, E Omidinia, Informatics in Medicine Unlocked Computational driven molecular dynamics simulation of keratinocyte growth factor behavior at different pH conditions. Informatics Med. Unlocked 23 (2021) 1-9.